

Home Unit Fuzzy Logic Controlled Single Stage Converter For Lithium-Ion (Li-Ion) Battery Charger for Electrical Vehicle

Ammar Issa Ismael, Ungku Anisa Ungku Amirulddin, Sabarina Jaafar

Department of Electrical Power Engineering, Universiti Tenaga Nasional, Malaysia.

Abstract: Recently, people are moving towards the use of electric vehicle transport compared to ordinary fuel consuming transportation. This is due to the increasing awareness to reduce the greenhouse gas emission generated from ordinary transportations. The main part of an electric vehicle is the battery and this battery requires charging as opposed to refueling in ordinary vehicles. A home unit charger is important to make EV applicable in all places where single-phase AC electrical points are available. Typically, Lithium Ion (Li-ion) batteries are charged by a two-stage converter topology. However, this paper proposes a Lithium-ion battery charger for an electrical vehicle constructed from a single stage boost converter topology, namely a phase shift semi-bridgeless boost converter. A Sugeno fuzzy logic controller is also designed to control the converter and manage the charging of the battery load (dynamic load) depending on the battery state of charge to achieve constant current (CC) constant voltage (CV) charging strategy. The results presented in this paper shows that the designed controller for the single-stage converter topology can successfully charge the Li-ion battery suitable for 400 V applications with low ripple voltage. The model is ideally suited for automotive level I residential charging applications.

Key words: home unit, PWM, battery charger, AC to DC converter, Sugeno fuzzy logic

INTRODUCTION

Presently, the transportation segment has become a great consumer of fossil fuels and donates enormously to global greenhouse gas (GHG) emissions (Gerssen-Gondelach & Faaij, 2012). In the year 2005, about 15% of global GHG releases had been from the transport segment, to which road transport contributes 73% (OECD/ITF, 2010). The greenhouse gas release is the main problem to the sustainability of the earth and it seriously affects humans, animals and plants. In order to overcome this problem, environmentally concerned companies are proposing to increase the use of electric vehicles (EV) in cities as opposed to the use of conventional vehicles (Van Mierlo, Maggetto, & Lataire, 2006). To ensure the success of adopting electric vehicles, owners must ensure their EVs are continuously charged. EV charging will normally take place at night where the EV can be plugged-in to a suitable mains outlet for Level 1 (slow) charging. Both private and public facilities can also employ level 2 charging as the primary method which requires a 240 V outlet (Yilmaz & Krein, 2013).

Two popular types of batteries used in battery powered electric vehicles (BEV) are nickel metal hydride (NiMH) and lithium-ion (Li-ion) (Pollet, Staffell, & Shang, 2012). Nowadays Lithium-ion batteries are becoming the common energy source for personal computers, mobile phones, electric bikes and in future for electrical cars too. But for the reason of severe safety issues, especially in mobile computer applications, high-performance Li ion batteries become disreputable (Kallfab, Hoch, Hilger, & Manke, 2012).

EV battery chargers are categorized in to two main categories, namely OFF-board (or standalone) and ON-board (or integrated) chargers. An ON-board battery charger has to be light in weight, have a high energy density, is small in size and capable of transporting high power with high efficiency so as to maximize the output and maximize the distance covered per charge. Ac-dc power conversion architecture is only suitable for lead acid batteries although large low frequency ripples are present in the output current. Conversely the two-stage ac-dc/dc-dc power conversion provides essential low frequency ripple rejection as shown in Fig.1 below. And so, the two-stage method is preferred for PHEV and EV battery chargers, where the power rating is moderately high, and lithium-ion batteries requiring low voltage ripple, are used as the main energy storage system (Musavi, Eberle, & Dunford, 2011; Petersen & Andersen, 2002).

The conventional topology is effective for low and medium power range, up to around 1kW. In power levels greater than 1kW, designers parallel semiconductors in order to deliver greater output power. Also at high power, the inductor volume becomes a challenging design issue (Musavi, Eberle, & Dunford, 2010). In this paper the charger employs the phase shift semi-bridgeless converter topology that can deliver effective performance at high power, fair in price and small in size due to its of single stage and has only two MOSFETs (Musavi, et al., 2011).

The more effectiveness method is valid for the design of the battery charger for which two charging states can occur; normal charging conditions and end of charge (Van Mierlo, et al., 2006). The battery charging algorithm is important for the development of the charger, it is required to reduce the charging time and stop overcharging. So the charging strategy employed is constant current (CC) at the start of charging with the battery voltage increasing

Corresponding Author: Ammar Issa Ismael, Department of Electrical Power Engineering, Universiti Tenaga Nasional, Malaysia.

from the present voltage until near the fully charged voltage, then transferring to constant voltage (CV) with decrease in the current until the current reaches zero at full battery charge.

This strategy can be achieved through a simple way without using complex mathematics through the use of fuzzy logic control which will be presented in this paper. The inputs to the fuzzy logic control will be the battery voltage and state-of-charge (SOC). The fuzzy logic controller will control the switching of the phase shift semi-bridgeless boost converter in the EV battery charger.

The paper is organized as follows. Section I presents the introduction while section II will explain the operation principle of the chosen converter topology. Then, the designed fuzzy logic control will be described in section III with the simulation results of the designed system presented in section IV. Finally, section V will provide the conclusions of the paper.

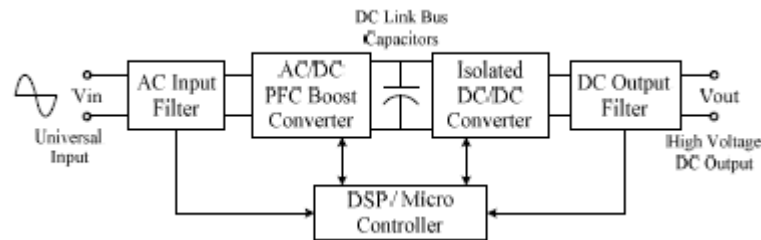


Fig. 1: Simplified block diagram of a two-stage universal battery charger.

II. The Operation Principle of the Converter Topology:

The conventional boost, bridgeless boost and interleaved boost topologies have disadvantages that are overcome by the phase shift semi-bridgeless boost converter topology shown in Fig.2 (Musavi, et al., 2011). This topology has high efficiency at light loads and low lines, which is critical to minimize the charger size, charging time and the amount and cost of electricity drawn from the utility; lower component count, which reduces the charger cost; and reduced EMI. The phase shift semi-bridgeless boost converter is suitable for automotive level I residential charging applications.

The topology has two additional slow diodes (D_a and D_b) to the bridgeless configuration which links the common point of the PFC with the input line. However, the current does not always return through these diodes, so their associated conduction losses are low. This occurs since the inductors exhibit low impedance at the line frequency, a large portion of the current flows through the FET intrinsic body diodes. In this topology, 180° out of phase are applied for the gating signals of the FETs.

To study the circuit operation, the input line cycle has been separated into the positive and negative half-cycles as described in sub-sections 1, 2 and 3 that follow. Furthermore, the circuit operation depends on the duty cycle, D , employed. Positive-half cycle operation study is provided for $D > 0.5$ in sub-section 3.

1. The operation during Positive-Half Cycle

During the positive-half cycle shown in Fig.3, the AC input voltage is positive, hence Q_1 turns on and current flows through L_1 and Q_1 and continues through Q_2 and then L_2 before returning to the line. Thus, storing energy in L_1 and L_2 . During the return process, part of the current will flow through the body-diode of Q_2 and through D_b back to the input.

2. The operation during Negative-Half Cycle

As shown in Fig.2, when the AC input voltage goes through the negative half-cycle, Q_2 turns on and current flows through L_2 and Q_2 and continues through Q_1 and then L_1 before returning to the line, hence storing energy in L_2 and L_1 . When Q_2 turns off, energy stored in L_2 and L_1 is released as current flows through D_2 , through the load and returns split between the body-diode of Q_1 and D_a back to the input.

3. Positive-Half Cycle Operation and Analysis for $D > 0.5$

The operation of the proposed converter also depends on the duty cycle employed. During any half cycle, the duty cycle of the converter is either bigger than 0.5 ($D > 0.5$) or less than 0.5 ($D < 0.5$). The step-by-step operation of the proposed converter for $D > 0.5$ is shown in Fig.3 to Fig.5 during the positive-half cycle. In the first step shown through Fig.3, when Q_1 and Q_2 are ON the input current passes through L_1 and L_2 to induce and store energy in the inductors with some passing through D_b to the source. At the same time, the capacitor bank will discharge into the load. When Q_1 is ON and Q_2 is OFF with diode of Q_2 not conducting, the L_1 will store most of the energy through Q_1 and some energy stored into L_2 through the body-diode of Q_2 . Consequently, the capacitor bank will discharge through the load as illustrated in Fig.4. The third step, as shown in Fig.5, occurs when Q_1 is OFF and Q_2 is ON. The energy from the source is released to the load through D_1 and return to the source through D_b with some of current returning to the source through Q_2 and L_2 .

From the positive-half cycle operation, it can be seen that for the negative-cycle, similar operation will occur but instead of D_b conducting, the diode D_a will conduct current and D_2 will release the energy to the load when Q_2 is OFF and Q_1 is ON. Also, during the negative-half cycle, similar operation will occur when Q_1

and Q2 are both ON. The body-diode of Q1 will conduct when Q1 is OFF and Q2 is ON in the negative-half cycle.

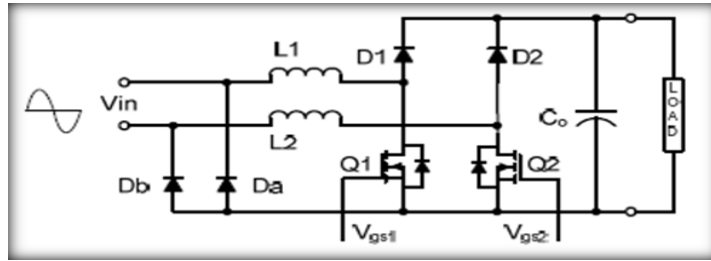


Fig. 2: Phase shifted semi-bridgeless PFC boost converter topology.

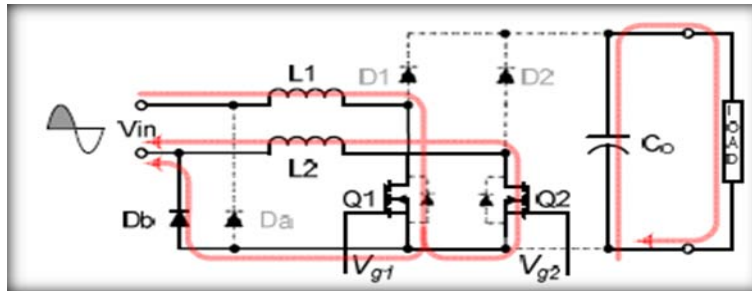


Fig. 3: Positive-half cycle operation with $D > 0.5$: Q1 and Q2 are both ON.

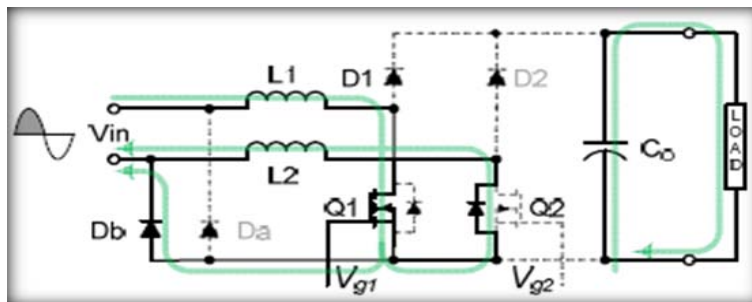


Fig. 4: Positive-half cycle operation with $D > 0.5$: Q1 ON and body-diode of Q2 conducting.

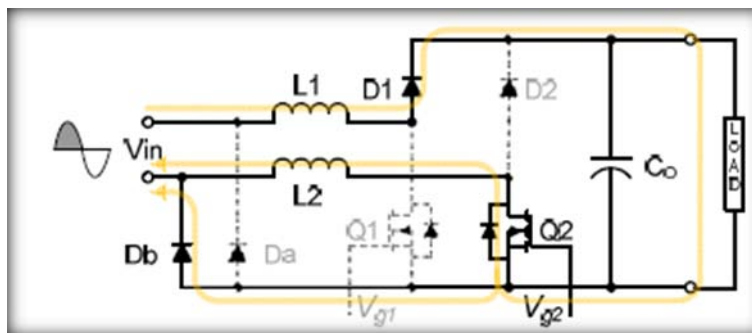


Fig. 5: Positive-half cycle operation with $D > 0.5$: Q1 OFF and Q2 ON.

Determining the values of inductors L1 and L2 depends on the amount of ripple of current present at the load. Since the charging of the Li-ion battery is very sensitive towards current ripple, therefore the converter was designed with $\Delta I = 0.2$. The values of L1 is determined using equation (1) for $D < 0.5$ and equation (2) for $D > 0.5$. The value of L2 is made equal to L1.

$$L1 \geq (1 / (2 * \Delta I)) * ((Vo - Vin) (0.5 - D) * Ts) \tag{1}$$

$$L1 \geq (1 / (2 * \Delta I)) * ((Vo - Vin) (1 - D) * Ts) \tag{2}$$

Where Vo is output voltage, Vin is input voltage..., and Ts is time sample

Thus, by using these two equations, Table 1 below presents the values of L1 and L2 calculated at different values of duty cycle, D. From Table 1, the most suitable value for L1 and L2 is found to be 9mH due to it occurring repeatedly when D is 0.1 and 0.6. However, from the simulation conducted, it was found that 10 mH was the most the suitable value for L1 and L2 for the designed fuzzy logic controlled battery charger.

Table 1: Calculated L1 and L2 values for different duty cycle, D.

D	0.1	0.2	0.3	0.4	0.49	0.51	0.6	0.7	0.75
L1, L2	9 mH	6.75mH	4.5mH	2.25mH	2.25mH	11mH	9mH	6.74mH	5.6mH

III. Design of the Sugeno Fuzzy Logic Control for the Phase Shifted Semi-Bridgeless Boost Converter:

This section will present the design of a Sugeno fuzzy logic controller to control the phase shifted semi-bridgeless boost converter to be used in charging a 108 cell Li-ion battery. The Li-ion battery is to be charged from 220 V (corresponding to 2.037 V/cell) up to 422 V (corresponding to 3.9V/cell). The controller is required to change the duty cycle of the boost converter to charge the battery up to the required voltage level while keeping the charging current constant. Therefore, the duty cycle will depend on the SOC of the battery and thus, for this reason, the Sugeno method was chosen since it enables the output of the fuzzy system to be dependent on the inputs of the fuzzy system. The two inputs to the designed fuzzy logic control for the battery charger are battery voltage (Vb) and battery state-of-charge (SOC).

The battery voltage input is divided into two membership functions; namely ‘charge’ and ‘full’, represented using ‘trapezoidal’ functions as illustrated in Fig.6 below.

Charge (a) is between 0 to 400, i.e. [0 – 400] (trapmf fun.).

$$\text{So, charge (a)} = \begin{cases} \frac{a}{10} & 0 \leq a \leq 10 \\ 1 & 10 < a \leq 380 \\ \frac{a-400}{-20} & 380 \leq a \leq 400 \end{cases} \quad (3)$$

The second input to the fuzzy logic which is the battery SOC can vary from 0 to 100%. From observation, there is a relationship between the duty cycle and charging current which also depends on the value of battery voltage. The initial battery voltage of 220 V is the same as the RMS voltage of the input supply. Therefore, the converter does not have to boost the input voltage during this instance and the duty cycle is adjusted close to zero. As the battery voltage increases, the duty cycle is increased in two stages, firstly linear and followed by nonlinear increase. Therefore, twenty membership functions were developed for the battery SOC input distributed from 10% to 100% SOC as shown in Fig. 7.

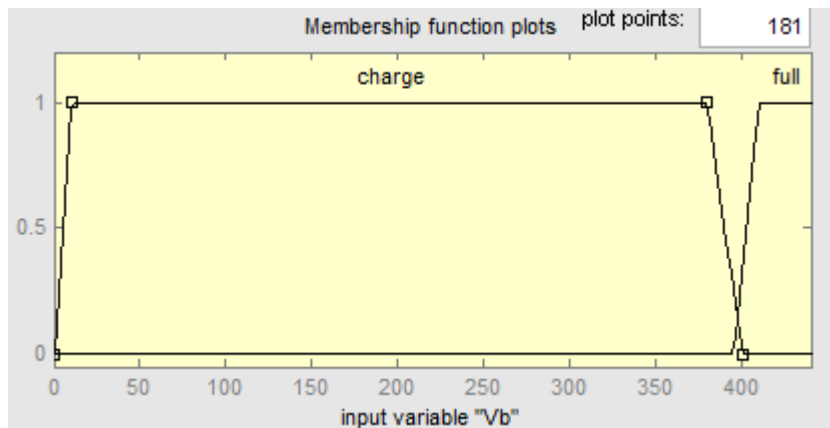


Fig. 6: Input membership functions for battery voltage.

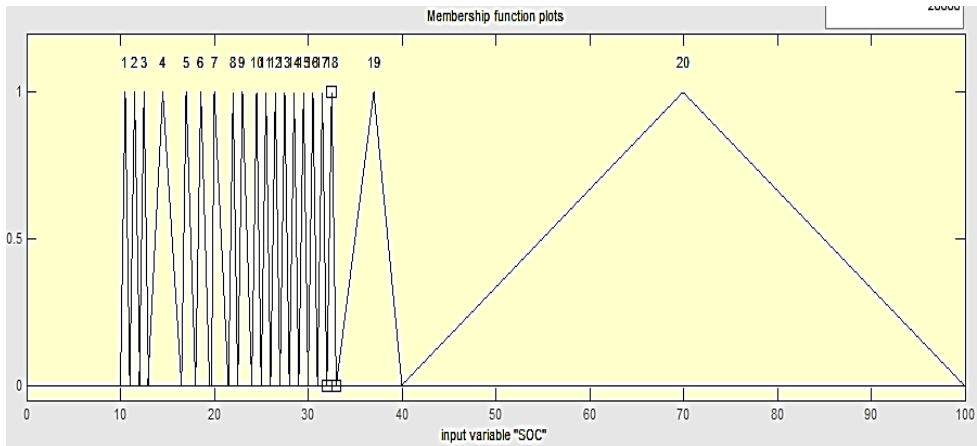


Fig. 7: Input membership functions for battery SOC.

The output of the designed fuzzy logic controller will be a number ranging from 0.0015 to 0.75. This will then be compared with a 20 kHz triangle wave to produce the gate voltage V_{g1} for MOSFET Q1 whilst gate voltage V_{g2} for MOSFET Q2 is produced from comparing the output of the fuzzy logic controller with the 180° phase shifted 20 kHz triangle wave.

As mention previously, the output of a Sugeno fuzzy logic system designed will depend on the input battery SOC, so the output function of the Sugeno fuzzy logic is a linear function adjusted to be relative to the value of battery SOC and independent of the battery voltage. The Sugeno linear output function has three constant parameters, a, b and c as shown in equation (4).

$$D (\text{output of Sugeno fuzzy logic}) = a \cdot x_1 + b \cdot x_2 + c \tag{4}$$

Where:-

x_1 is first input of fuzzy logic, x_2 is second input of fuzzy logic and In equation (4), a, b and c are constant values. In the designed fuzzy logic control, $a = c = 0$, and b is adjusted depending on each level of battery SOC as shown in Table 2.

Table 2: Values of c with respect to output membership functions of the designed Sugeno fuzzy logic control.

Membership functions of output	values of c	Membership functions of output	Values of c
1	0.0015	9	0.024
2	0.0175	10	0.025
3	0.031	11	0.0219
4	0.03	12	0.0218
5	0.033	13	0.42(constant)
6	0.035	14	0.034
7	0.032	15	0.4(constant)
8	0.028		

IV. Simulation Results of the Designed Fuzzy Logic Controlled Boost Converter for Li-Ion Battery Charging:

Fig. 8 shows the designed fuzzy logic controlled phase shifted semi-bridgeless boost converter to charge a Li-ion battery. An inductance L_3 of 5mH is added in series with the battery to reduce further the current ripple. A diode is also added in series to the battery to ensure that the battery does not discharge through the converter. The battery voltage and battery SOC are feedback to the designed fuzzy logic control as shown in Fig. 9. At any SOC, the duty cycle given by the fuzzy logic output is halved during the start of the charging process, using the relay switch shown in Fig.9, to limit the charging current at the start. After that, the relay switch will revert to the actual fuzzy logic output to maintain constant charging current constant from the starting 10.5% battery SOC, corresponding to battery voltage of 220 V until the battery voltage reaches 395 V. Then the current starts to reduced and voltage kept approximately constant until the converter stops the charging at 422 V.

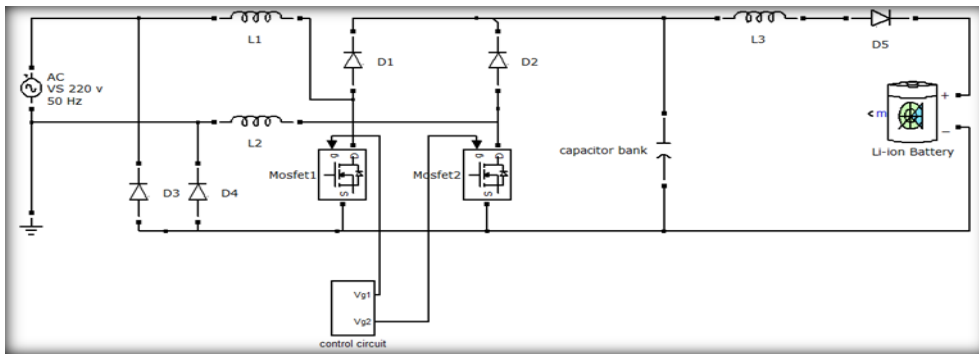


Fig. 8: Phase shift semi-bridgeless boost converter topology with the designed fuzzy logic control connected to charge a Li-ion battery load.

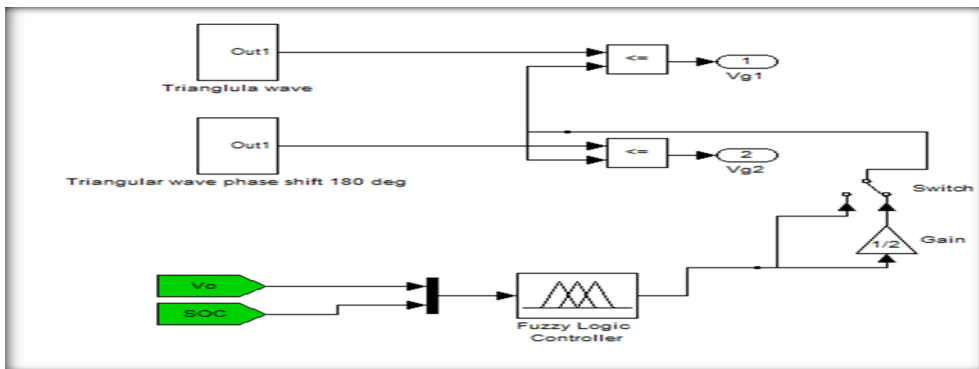


Fig. 9: Designed fuzzy logic control circuit to produce the gate voltages of the MOSFETs in the battery charging system shown in Fig. 8.

Fig. 10 shows the input current to the converter. From the simulation results, the charging current was seen to settle at a fixed value of 18 A with small ripple as shown in Fig. 11(a) with a starting battery SOC of 10.5%. The high current ripple at the start of the simulation was attenuated by the inductor L3 connected in series with the battery Fig. 11(b) shows the battery voltage obtained from the simulation with a starting battery voltage of 10.5%. The rise in battery voltage seen in Fig. 11(b) shows that the designed fuzzy logic controlled phase shifted semi-bridgeless boost converter is able to charge the battery and increase its SOC.

As mentioned previously, the duty cycle is initially halved at the start the charging process to avoid high starting current especially when the charger starts to charge the battery under high battery SOC conditions as shown in Fig.12 (a). Fig. 12(a) also shows that the designed battery charger is able to maintain the charging current at 18 A even with a starting battery SOC condition of 12.5 % similar to the case with 10.5% initial battery SOC. The corresponding battery voltage was found to increase from 261.25 V as illustrated in Fig.12 (b), hence, increasing the battery SOC from the initial 12.5%.

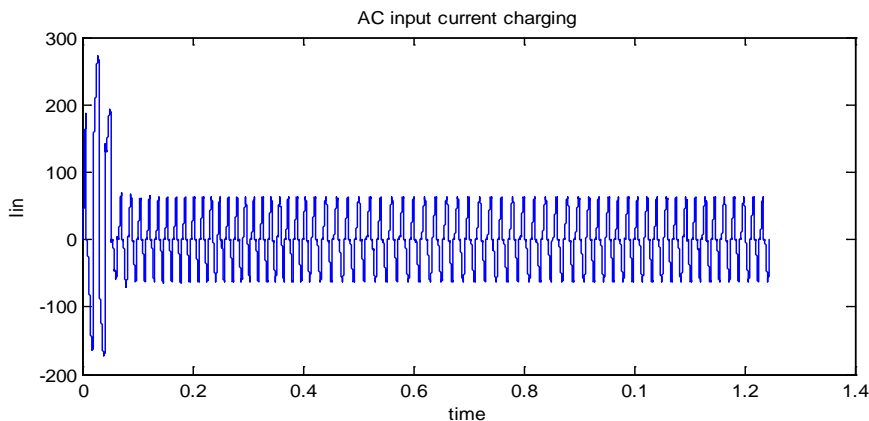


Fig. 10: AC input current charging for battery load.

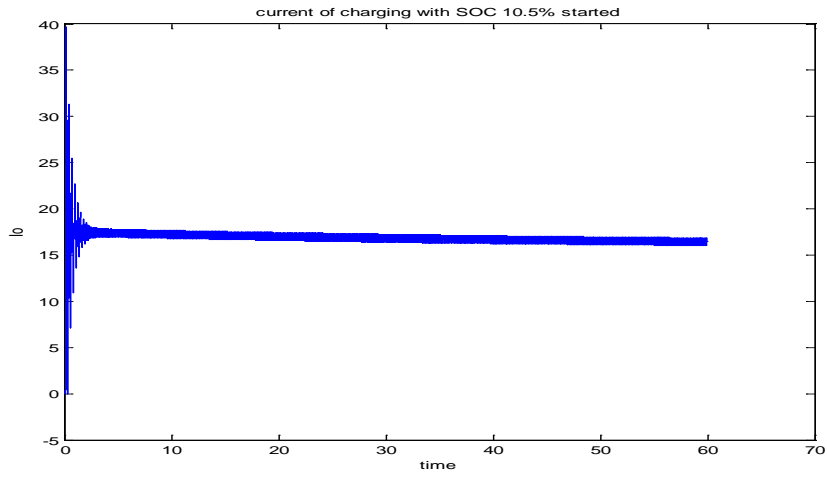


Fig. 11(a): Charging current obtained from simulation with initial battery SOC of 10.5%.

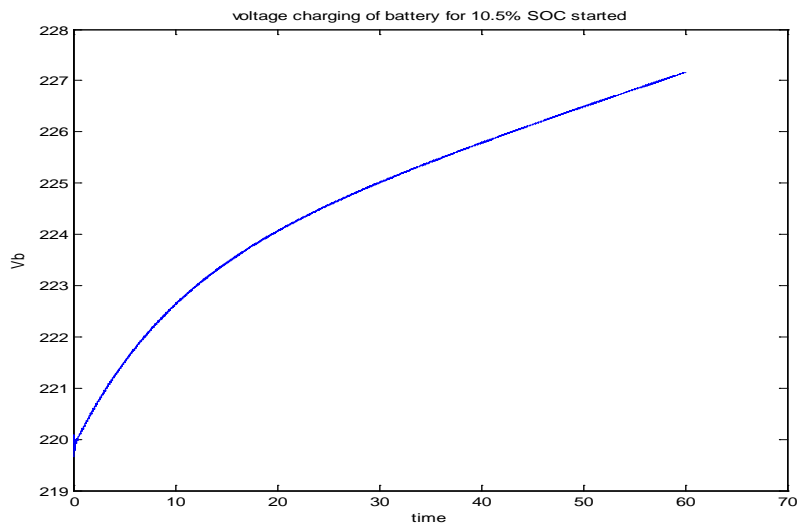


Fig. 11(b): Battery voltage obtained from simulation with initial battery SOC of 10.5%.

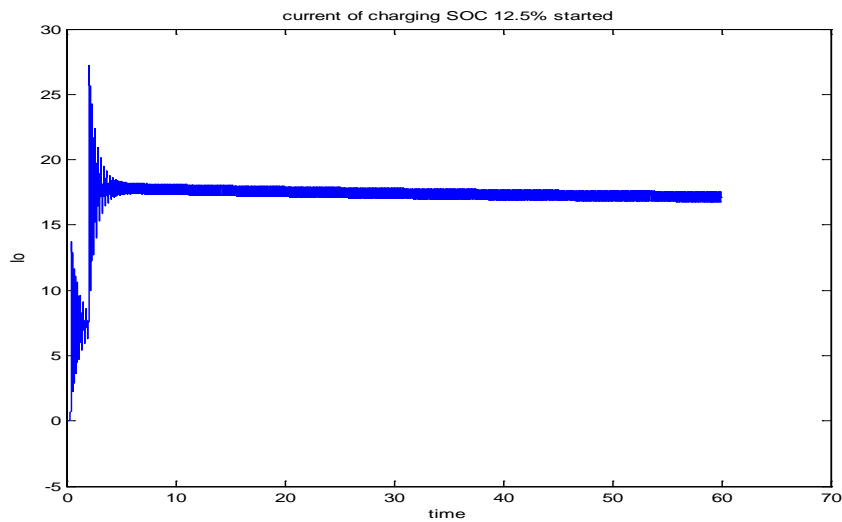


Fig. 12(a): Charging current obtained from simulation with initial battery SOC of 12.5 %

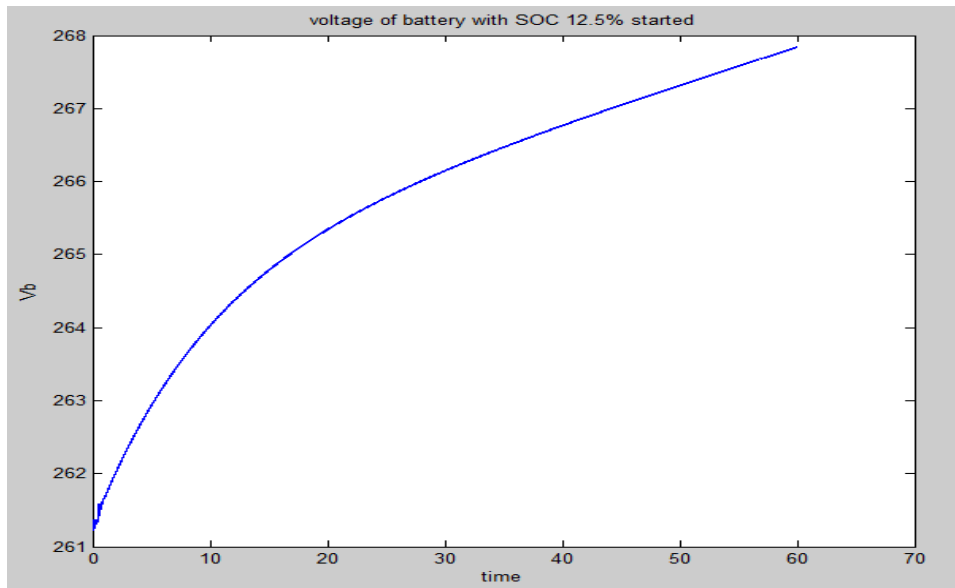


Fig. 12(b): Battery voltage obtained from simulation with initial battery SOC of 12.5 %.

When the voltage of the battery reaches 395 V, the current decreases until it reaches zero and battery voltage becomes 422 V which is the maximum value at 100 % of SOC. This corresponds to the second stage of the battery charging strategy which is the constant voltage condition. This is achieved by controlling the duty cycle of the MOSFETs depending on the battery voltage and battery SOC with fuzzy rules set in place to ensure safe charging. The decrease in charging current and constant battery voltage is seen in Fig.13 (a) and Fig. 13(b) for initial battery SOC of 33%.

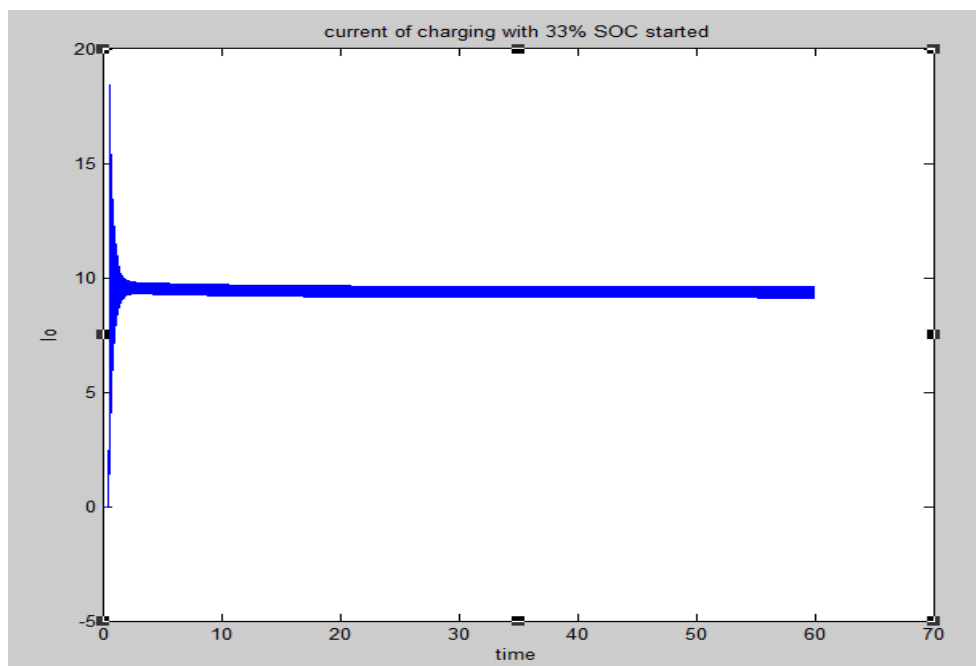


Fig. 13(a): Charging current obtained from simulation with initial battery SOC of 33%.

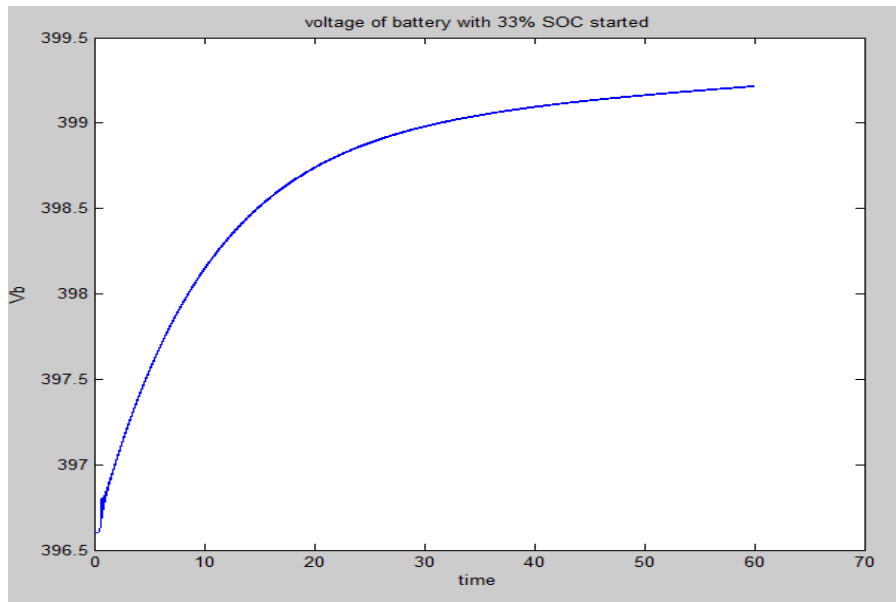


Fig. 13(b): Battery voltage obtained from simulation with initial battery SOC of 33%.

V. Conclusion:

The results presented in this paper has shown that the designed fuzzy logic controlled phase shift semi-bridgeless boost converter was able to increase the battery voltage, and hence charge the battery, continuously until the battery reached the desired voltage by varying the duty cycle of the converter from zero to 0.75. The designed battery charging system was able to maintain constant current of 18 A during the charging process from the initial voltage of 220V until the battery reached 395 V. Then, the designed system was able to switch into the constant voltage strategy to continue charging the battery from 395 V until it is fully charged at 422 V with the charging current reducing to zero.

This process was achieved using the designed Sugeno fuzzy logic control which allowed the output of the fuzzy to depend on the battery SOC fuzzy input. . The designed system charged the battery from an initial battery voltage of 220V, corresponding to 10.5% SOC, which is the same as the RMS voltage of the supply. If the battery is to be charged from a lower initial battery SOC, then the it is proposed that a buck converter circuit to be added in parallel to the designed boost converter presented in this paper.

APPENDIX

-System parameters:

$L1=L2=10$ mH, $L3= 5$ mH, $C_{bank}=22$ mF, *input AC voltage*=220V RMS, *input voltage frequency*=50Hz.

ACKNOWLEDGMENT

I would like to thank Prof. **Saad Mekhilef** and **Dr. Mahmoud A.A. Younis**, their emphasis on minute details have been instrumental in successfully completing this study.

REFERENCES

- Gerssen-Gondelach, S.J., A.P. Faaij, 2012. Performance of batteries for electric vehicles on short and longer term. *Journal of power sources*, 212: 111-129.
- Kallfab, C., C. Hoch, A. Hilger, I. Manke, 2012. *Short-circuit and overcharge behaviour of some lithium ion batteries*. Paper presented at the Systems, Signals and Devices (SSD), 2012 9th International Multi-Conference on.
- Musavi, F., W. Eberle, W.G. Dunford, 2010. *Efficiency evaluation of single-phase solutions for AC-DC PFC boost converters for plug-in-Hybrid electric vehicle battery chargers*. Paper presented at the Vehicle Power and Propulsion Conference (VPPC), 2010 IEEE.
- Musavi, F., W. Eberle, W.G. Dunford, 2011. *A phase shifted semi-bridgeless boost power factor corrected converter for plug in hybrid electric vehicle battery chargers*. Paper presented at the Applied Power Electronics Conference and Exposition (APEC), 2011 Twenty-Sixth Annual IEEE.
- OECD/ITF, 2010. Reducing Transport Greenhouse Gas Emissions. Trends and Data. 2011, from <http://www.internationaltransportforum.org/Pub/pdf/10GHGTrends.pdf>.

Petersen, L., M. Andersen, 2002. *Two-stage power factor corrected power supplies: The low component-stress approach*. Paper presented at the Applied Power Electronics Conference and Exposition, 2002. APEC 2002. Seventeenth Annual IEEE.

Pollet, B.G., I. Staffell, J.L. Shang, 2012. Current status of hybrid, battery and fuel cell electric vehicles: From electrochemistry to market prospects. *Electrochimica Acta*, 84: 235-249.

Van Mierlo, J., G. Maggetto, P. Lataire, 2006. Which energy source for road transport in the future? A comparison of battery, hybrid and fuel cell vehicles. *Energy Conversion and Management*, 47(17): 2748-2760.

Yilmaz, M., P.T. Krein, 2013. Review of Battery Charger Topologies, Charging Power Levels, and Infrastructure for Plug-In Electric and Hybrid Vehicles. *Power Electronics, IEEE Transactions on*, 28(5): 2151-2169.